Received: 10 August 2021 | Revised: 12 December 2021 | Accepted: 13 December 2021

DOI: 10.1002/gj.4384

RESEARCH ARTICLE

WILEY

Distinguishing the Miocene Kiel and Antwerpen Members (Berchem Formation) and their characteristic horizons using cone penetration tests in Antwerp (northern Belgium)

Jef Deckers[1] | Stijn Everaert[2]

[1]VITO, Mol, Belgium

[2]Aalst, Belgium

Correspondence
Jef Deckers, VITO, Boeretang 200, 2400 Mol, Belgium.
Email: jef.deckers@vito.be

Handling Editor: I. D. Somerville

The glauconitic sands in the upper part of the lower-middle Miocene Berchem Formation are subdivided into the Kiel and Antwerpen Members. Although lithological differences between both members are well known from temporary outcrops in the Antwerp city area, they are difficult to distinguish in boreholes, which hinders regional mapping of these units. In this study, we investigate whether both members can be distinguished on cone penetration tests (CPTs). For this purpose, we correlated multiple outcrops—in which the Kiel and/or Antwerpen Members have been identified—with nearby CPTs. On the CPTs, the boundary between the Kiel and Antwerpen Members is clearly identifiable as it coincides with an abrupt upwards decrease in cone resistance (q_c). The lower q_c of the basal part of the Antwerpen Member is probably related to the finer grain size with more clayey admixture compared to the underlying Kiel Member. This change to a finer grain size is caused by a decrease in depositional energy and sedimentation rates as the region was transgressed during the eustatic sea-level rise at the start of the Mid-Miocene Climatic Optimum. On the CPTs, several spikes in q_c values were observed within the Antwerpen and Kiel Members. These spikes could be correlated to shell beds, three horizons with sandstones and possibly a hardground. The sandstones appear to be discontinuous, whereas some of the shell beds could be traced across the entire study area. Most shell beds probably represent storm deposits within an otherwise relatively low energetic sedimentary environment. A phosphatic shell bed above the base of the Antwerpen Member is interpreted as the maximum flooding surface, lying in a zone with the lowest q_c values for the Antwerpen Member, which might reflect maximum fining. The shell beds and interlayered sands of the Antwerpen Member thin in a southern direction, indicating reduced accommodation space in this direction.

KEYWORDS
cone penetration tests, early unconformity, Miocene, North Sea Basin, shell beds, stratigraphy

1 | INTRODUCTION

The glauconitic sands of the Berchem Formation were deposited during the early and middle Miocene (Louwye, De Coninck, & Verniers, 2000) in the southern North Sea Basin (Figure 1). The sands are green to blackish due to their high glauconite content, they are fine- to medium fine-grained, often slightly clayey, and rich in shells (De Meuter & Laga, 1976). Sandstone pebbles and phosphorite

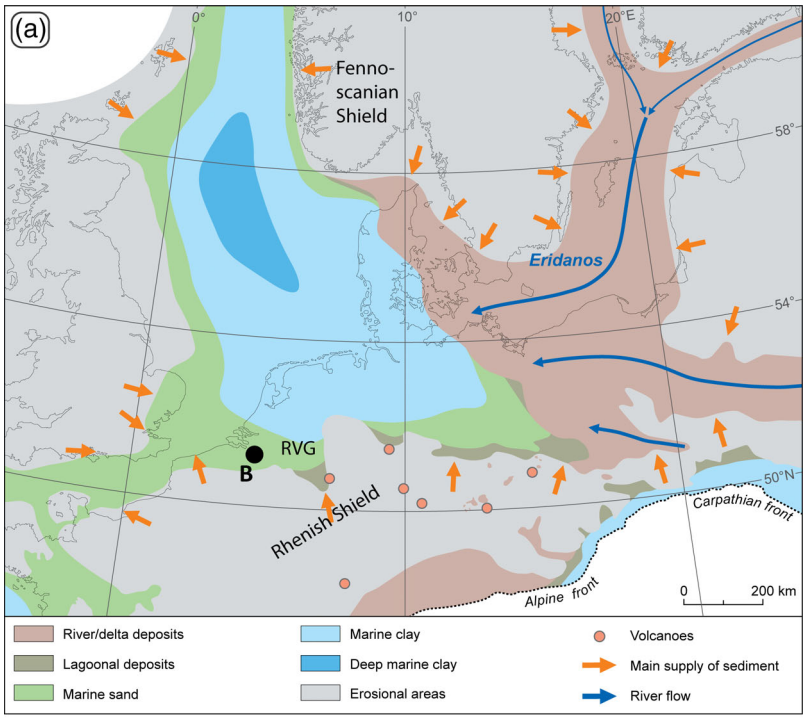

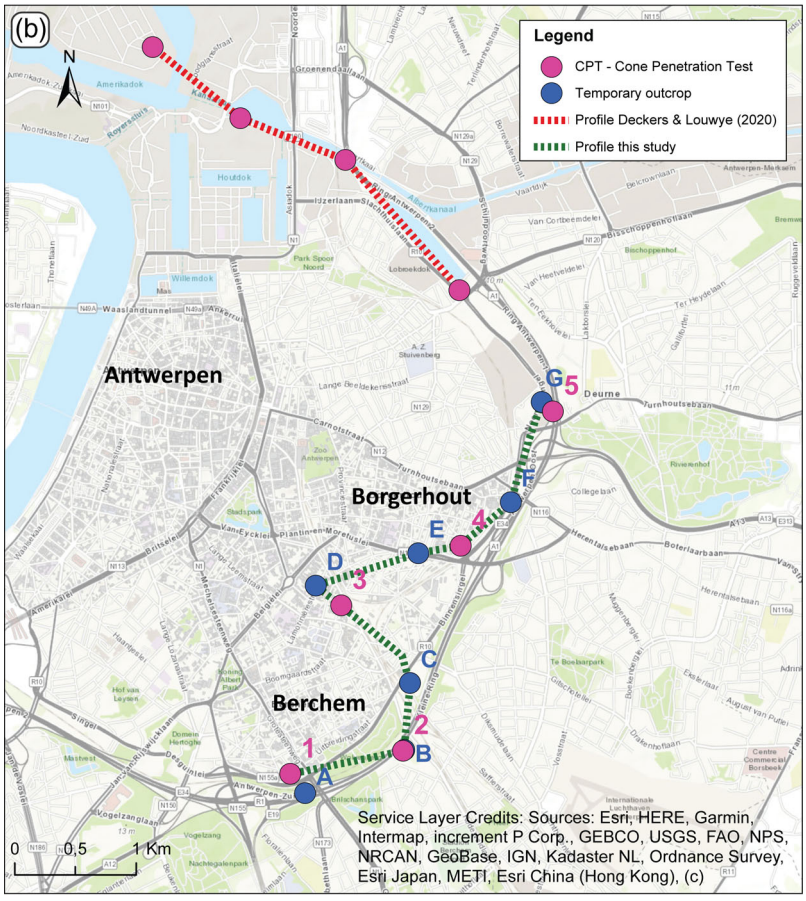

FIGURE 1 (a) The Middle Miocene (late Langhian) palaeogeography of the North Sea Basin and surrounding areas, modified from Gibbard and Lewin (2016) and Deckers and Munsterman (2020). (b) Overview of the study area with the correlation profile of Deckers and Louwye (2020; Figure 4) along the northern Antwerp city area and the correlation profile of this study (Figures 5, 9, and 10) along the eastern Antwerp city area. A = Berchem-Grote Steenweg (A.G.; GSB 028w0397; DOV kb15d28w-B451); B = Posthofbrug (DOV TO-20100101); C = Post X (GSB 028e0923; DOV TO-20150701); D = Argenta (GSB 028w1004; DOV TO-20190417); E = Tweelingenstraat (GSB 028e0922; DOV TO-20191211); F = Borgerhout-Stenen Brug (I.S.B.; GSB 028e0497; DOV kb15d28e-B578); G = Borgerhout-Rivierenhof (XI B.R.; GSB 028e0499; DOV kb15d28e-B580); 1 = GEO-03/146-S4; 2= GEO-68/101-SVII; 3= GEO-96/120-S2; 4= GEO-03/146-S15BIS; 5= GEO-07/154-S11

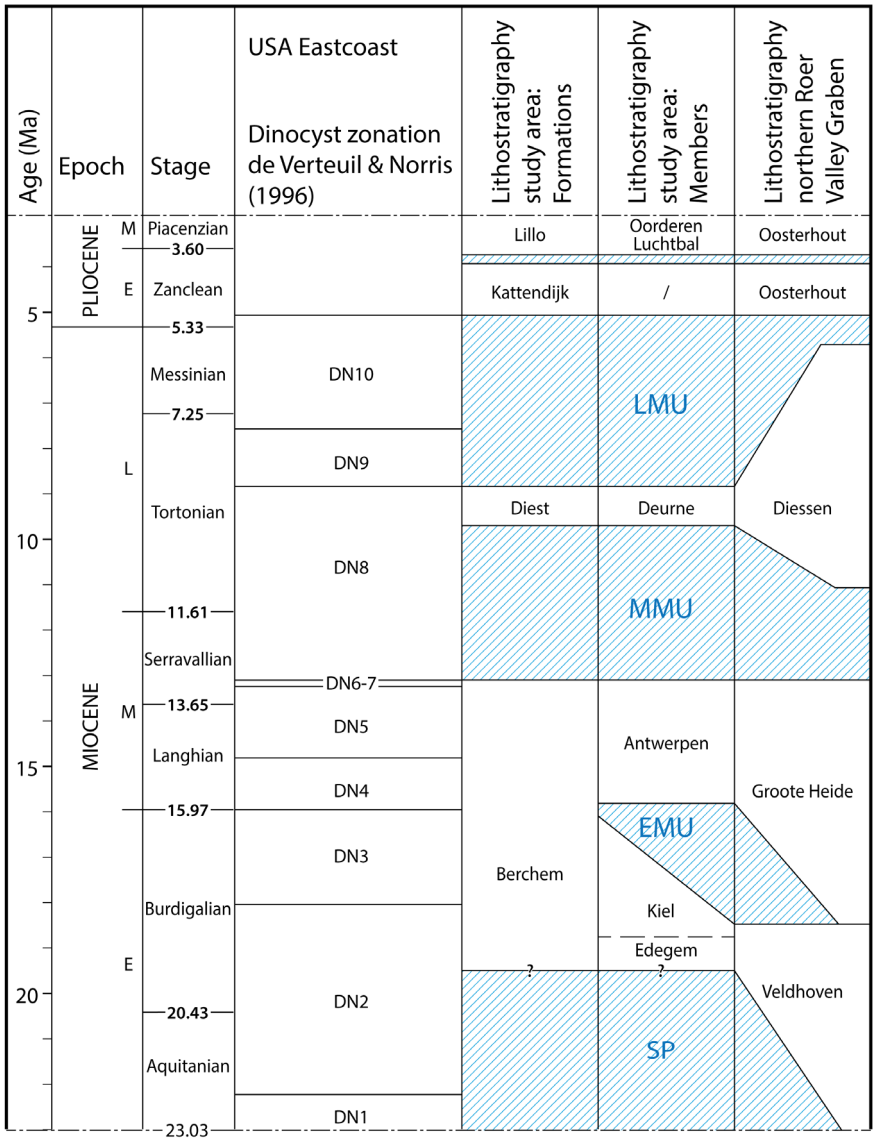

FIGURE 2 The litho- and chronostratigraphic framework of the Neogene in the study area. The chronostratigraphy and correlation with the dinocyst zonation scheme of de Verteuil and Norris (1996) are based on Figure 6 of Dybkjær and Piasecki (2010). The ages of the stratigraphic successions in the northern Roer Valley Graben are based on Munsterman et al. (2019). The ages and zonation of the Belgian units follow Vandenberghe and Louwye (2020) and Everaert et al. (2020) for the Kiel Member. As the biostratigraphic transition between the Edegem and Kiel Members is yet under discussion, the age of their boundary is indicated by a dashed line. The base of the Edegem Member and Berchem Formation is marked with a question mark; although Munsterman and Deckers (2020) were able to identify Aquitanian strata (based on dinocyst analyses) in the very base of the Berchem Formation in the Mol and Weelde boreholes, this remains uncertain for the Antwerp area. SP, Savian phase; EMU, Early Miocene Unconformity; MMU, Middle Miocene Unconformity; LMU, Late Miocene Unconformity

nodules are present at different levels, and several shell beds or crags are recognized. Within the Antwerp type area of the Berchem Formation, three of its members were described in temporary outcrops by De Meuter, Wouters, and Ringele (1976) and formalized by De Meuter and Laga (1976), from base to top called the Edegem, Kiel, and Antwerpen Members (Figure 2).

The central Kiel Member forms a particular unit of the Berchem Formation, as its rather coarse sands often lack fossils due to strong decalcification in its type area, southern Antwerp (De Meuter & Laga, 1976). Recent studies have, however, shown that the Kiel Sands contain some (fragile) shell beds to the north of the city (De Schutter & Everaert, 2020; Everaert et al., 2020). In the central and northern Antwerp city area, the Kiel Member is covered by the fossiliferous Antwerpen Member. In several temporary outcrops in and around the city of Antwerp, the boundary between the Antwerpen and Kiel Members was described in great detail and illustrated by De Meuter et al. (1976), Louwye, Marquet, Bosselaers, and Lambert (2010), Hoedemakers and Dufraing (2018), De Schutter and Everaert (2020) and Everaert et al. (2019, 2020). The latter authors indicated that the Antwerpen Member appears finer grained and more clayey in the basal parts compared to the underlying Kiel Member. In addition, a notable colour difference can be observed in temporary outcrops, as the dark green to blackish Antwerpen Member contrasts with the more greyish Kiel Member (Figure 3). Especially in dry profiles, this colour difference can be striking. In nearby boreholes, on the contrary, the lithological differences between the latter units were generally too subtle to make a distinction between them. Consequently, the Kiel Member was hardly identified in boreholes in the subsurface of Flanders and mapped together with the overlying Antwerpen Member in geological models (Deckers et al., 2019; Van Haren et al., 2021). The boundary between the Antwerpen and Kiel Members, nevertheless, has regional significance as its timing coincides with the Early Miocene Unconformity (EMU) in the southern North Sea Basin, as defined by Munsterman et al. (2019).

In a recent study of the architecture of the Kattendijk Formation on cone penetration tests (CPTs), Deckers and Louwye (2020) showed

that two geotechnical units could be distinguished within the upper Berchem Formation, without discussing their lithostratigraphic significance (Figure 4). CPTs are present throughout the Antwerp city area and available near several published outcrops of the Antwerpen and Kiel Members and might therefore provide an excellent opportunity to study the geotechnical expressions of these members. These geotechnical expressions can in turn provide information on the boundary between the Antwerpen and Kiel Members and a better insight on the lower to middle Miocene sedimentary transition in the southern North Sea Basin.

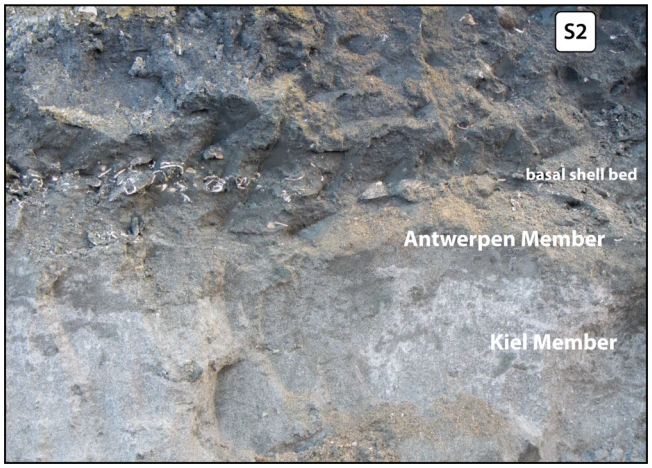

FIGURE 3 The boundary between the Antwerpen and Kiel Members in the temporary Argenta outcrop. Notice that the dark green to black colour of the Antwerpen Member contrasts with the more greyish Kiel Member. Photo by Taco J. Bor (November 2018). The figured succession is just over 1-m thick

2 | DATA SET AND METHODOLOGY

2.1 | Outcrops

First, a selection was made of temporary outcrops described in the literature, in which the boundary between the Antwerpen and Kiel Members—or a thick section of the Antwerpen Member—was established. A total of seven outcrops was selected along a more or less S-N line to the east of the city of Antwerp. These outcrops include some older sections exposed in the 1960s during the construction of the Antwerp Ring Road (De Meuter et al., 1976; Berchem-Grote Steenweg, Borgerhout-Stenen Brug and Borgerhout-Rivierenhof), and more recent temporary outcrops described by Louwye et al. (2010; Posthofbrug), Everaert et al. (2019; Post X), De Schutter and Everaert (2020; Argenta) and Everaert et al. (2020; Tweelingenstraat and a synthesis of the Argenta and Post X sections).

After selection, the lithostratigraphic interpretations and characteristic layers, that is, shell beds, horizons with sandstones, and hardgrounds were correlated by this study. This resulted in the correlation profile of Figure 5. Among the Post X, Argenta, and Tweelingenstraat outcrops, the correlations were based on those already performed by Everaert et al. (2020). The latter were extended for this study towards the other outcrops. Since the temporary outcrops studied by De Meuter et al. (1976) disappeared, the correlation of characteristic beds within these older outcrops remains tentative, especially higher up in the Antwerpen Member.

For the old Borgerhout—Stenen Brug outcrop, the correlations of characteristic layers also necessitated a revision of the lithostratigraphic interpretations of the lower part of the Antwerpen Member by De Meuter et al. (1976; Figure 6).

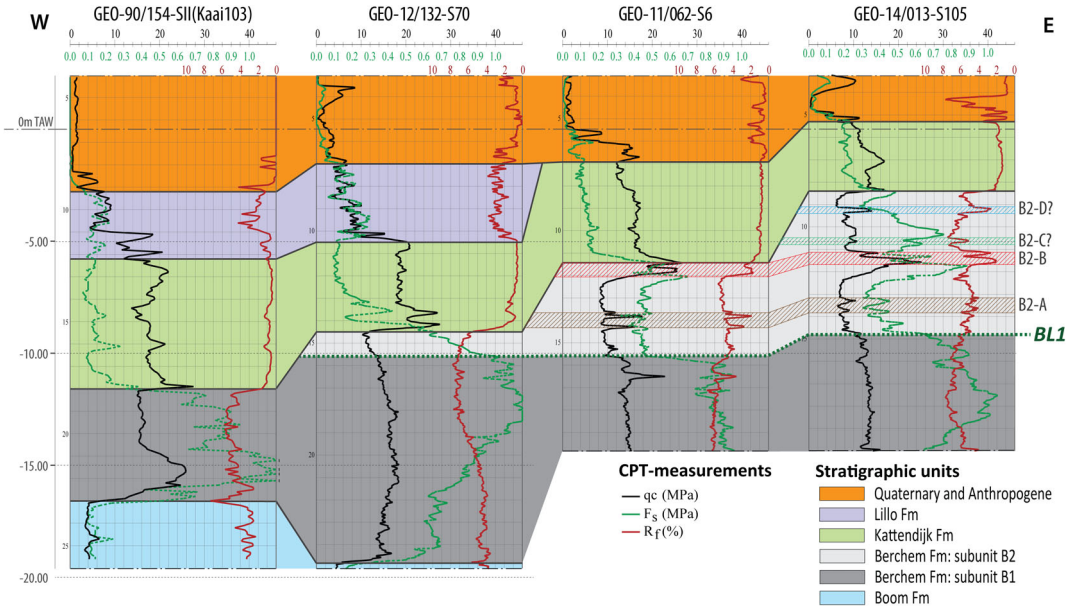

FIGURE 4 Part of the W-E correlation profile of the lower Oligocene to Quaternary units north of the city of Antwerp based on CPTs, modified after Deckers and Louwye (2020). The latter authors provided a geotechnical twofold subdivision of the Berchem Formation (subunits B1 and B2) that was also observed along the correlation panel of this study along the east of the Antwerp city area (Figure 9). B2-A to -D were added to this profile based on the results of this study. For the location of this profile, see Figure 1

Figures 7 and 8 provide photographs of some of the important boundaries, horizons, or features from the above-mentioned outcrops.

2.2 | Cone penetration tests

In the next step, CPTs were selected near or in between the outcrops. Over traditional methods of field investigation, the CPT has the advantage to be repeatable and economical in soft soils and to provide nearly continuous data. A CPT consists of pushing a tube with a cone-shaped head into the ground at a constant rate. Both the resistance of the cone tip to penetration (cone resistance or q_c) and the friction along a surface sleeve just above the cone tip (sleeve friction or f_s) are continuously monitored. From the latter variables, the friction ratio (R_f) can be calculated ($R_f = f_s/q_c \times 100\%$).

The preference went to electric CPTs and only if these lacked, mechanical CPTs were selected. Another selection criterion was the penetration depths of the CPTs as they had to reach at least the depths of the top of the Kiel Member. A total of five CPTs was selected, three of which are electric and two mechanical. A more or less S-N correlation profile was made between the selected CPTs (Figure 9). On the CPTs, we first interpreted the different lithostratigraphic units. Units or characteristic layers within the Berchem Formation with similar q_c and—if present—R_f were then identified, correlated between the selected CPTs, and labelled, leading to a geotechnical stratigraphy.

2.3 | Correlations between data sets

In a final step, the CPT units of Figure 9 were correlated with the lithostratigraphic outcrop interpretations of Figure 5 in order to compare the geotechnical characteristics and stratigraphy with the lithological characteristics and lithostratigraphy. The overview of this correlation is shown in Figure 10. Figures 11 and 12 provide a closer look into the correlations for the Argenta and Borgerhout-Rivierenhof outcrops.

Outcrop locations and interpretations were inventoried by De Nil, De Ceukelaire, and Van Damme (2020) and were together with the raw CPT measurement extracted from the public DOV database of Flanders (https://www.dov.vlaanderen.be), northern Belgium. For this study, all data were repositioned in reference to the 0 m TAW level (TAW: Belgian Ordnance Datum). Note that the CPTs and outcrops are not located at exactly the same spot, but near to each other, which may explain some of the small differences in depth between the boundaries on the CPTs and those described in the outcrops. The distance between the CPTs and nearby outcrops is indicated in Figure 10.

From most of the outcrops, samples were taken for dinoflagellate cyst analyses by Louwye et al. (2000, 2010) and Everaert et al. (2020). The latter studies all made use of the dinocyst zonation by de Verteuil and Norris (1996), which will therefore also be used for this study. In Everaert et al. (2020), this zonation was recalibrated to the time scale of Ogg, Ogg, and Gradstein (2016) and compared to the southern North Sea Miocene zonation of Munsterman and Brinkhuis (2004), to allow correlation with Dutch units. For the Argenta and Borgerhout-Rivierenhof outcrops, both representing the most complete sequences of the Kiel and Antwerpen Members, respectively, the results of the dinoflagellate cyst analyses by Everaert et al. (2020) and Louwye et al. (2000) are shown in Figures 11 and 12.

3 | OUTCROP CORRELATIONS

The selected outcrops generally expose a maximum of 10 m of the Berchem Formation below the Quaternary or Pliocene strata (Figures 5–8). The base of the Berchem Formation (Edegem Member) was not reached in any outcrop. In these outcrops, the Antwerpen and/or Kiel Members were interpreted and several particular layers within them, such as shell beds, horizons with sandstones, or hardgrounds. For the purpose of this study, the main horizons with sandstones, hardgrounds, and shell beds are marked in Figure 5 and referred to by Z, H, and S, respectively.

The base of the Antwerpen Member generally consists of 5–20 cm of slightly clayey glauconitic sand almost lacking shells, underlying a thin *Glycymeris* shell bed (Figure 3). Small, rare reworked sandstone clasts sometimes occur scattered at the base, but their concentration strongly differs between different outcrops (e.g., Everaert et al., 2020; Hoedemakers & Dufraing, 2018).

Three horizons with sandstones were identified in the outcrops, herein referred to as Z1 to Z3:

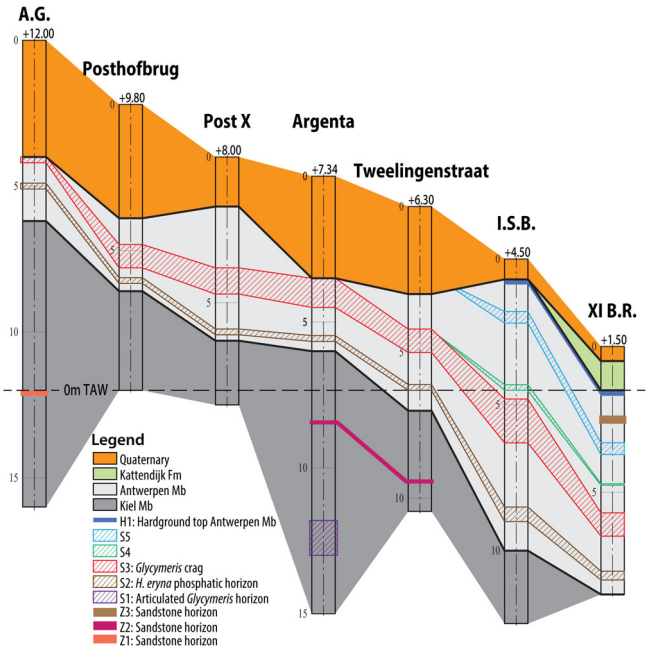

FIGURE 5 S-N correlation profile between lithostratigraphically (re)interpreted temporary outcrops along the east of the city of Antwerp. Besides the lithostratigraphy, also a correlation was made of some of the main shell beds, horizons with sandstones, and a hardground. A.G. = Berchem-Grote Steenweg; I.S.B. = Borgerhout-Stenen Brug; XI B.R. = Borgerhout-Rivierenhof. For the location of the outcrops, see Figure 1

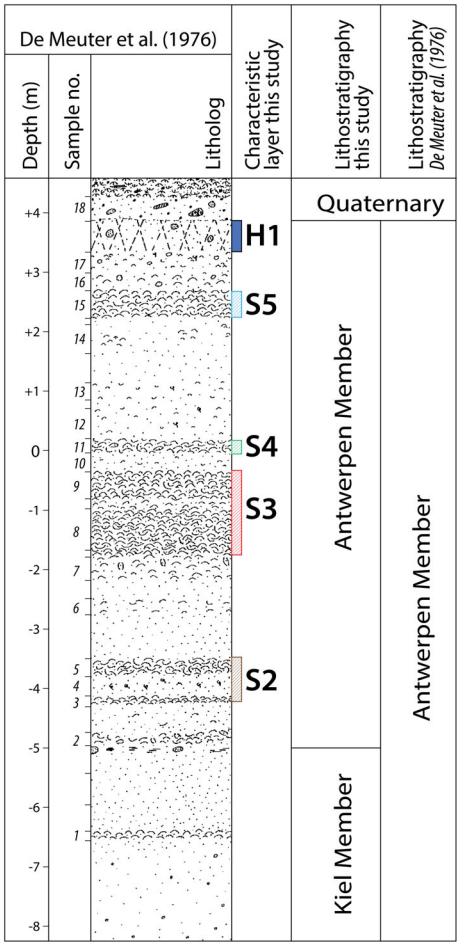

FIGURE 6 Revision of the lithostratigraphic interpretation by De Meuter et al. (1976) of the Borgerhout-Stenen Brug outcrop by this study. The codes of the characteristic layers of this study are also indicated. For the location of the outcrop, see Figure 1. H, hardground; S, shell bed

- Z1: In the Berchem-Grote Steenweg outcrop, about 6 m below the top of the Kiel Member, a level with "locally very friable shell fragments preserved in clay streaks and sandstones" was described by De Meuter et al. (1976). According to Louwye et al. (2000), this level represents the top of the early-middle Burdigalian dinocyst biozone DN2 in this section. The overlying higher parts (6 m) of the Kiel Member were attributed to the late Burdigalian zone DN3.
- Z2: In the Argenta and Tweelingenstraat outcrops, about 2.5 m below the top of the Kiel Member, another (1–15 cm thick) calcareous, glauconitic sandstone level was described by De Schutter and Everaert (2020) and Everaert et al. (2020). Especially at the Argenta outcrop, this sandstone bed, with short interruptions, was often massive and contained a thanatocoenosis of worn *Glycymeris* in its top surface (Figure 8b,c). These sandstone slabs were overlying a thin (usually 5–15 cm) shell bed with many large, worn, and convex-up oriented *Glycymeris baldii* (Glibert & Van de Poel, 1965) and *Cyrtodaria angusta* (Nyst & Westendorp, 1839) (Figure 8a). This shell bed and the sandstone horizon cannot be considered unrelated in further (geotechnical) interpretations. Both levels were attributed to the early-middle Burdigalian dinocyst biozone DN2 in Everaert et al. (2020). The top of dinocyst biozone DN2 was located ca 2 m higher in the profile (Figure 11).
- Z3: In the uppermost part of the Antwerpen Member in the Borgerhout-Rivierenhof outcrop, just 1 m below the boundary with the Kattendijk Formation, a thin shell bed with "sandstones" was described by De Meuter et al. (1976; Figures 5 and 12). This upper interval of the Antwerpen Member was tentatively assigned to the early-middle Serravallian DN6-DN7 zones by Louwye et al. (2000), which was later reaffirmed by Louwye, Deckers, Verhaegen, Adriaens, and Vandenberghe (2020).

Several shell beds were identified, herein referred to as S1 to S5:

- S1 is the lowermost shell bed, informally named "articulated *Glycymeris* horizon" (Figure 11). Due to its low stratigraphic position within the Kiel Member, it was only observed in the Argenta outcrop (De Schutter & Everaert, 2020; Everaert et al., 2020). It consists of more than 1 m of dispersed articulated valves of *Glycymeris* in life position. This level was attributed to dinocyst biozone DN2 by Everaert et al. (2020). However, its relative position within this biozone remains debated, as some late Aquitanian marker taxa were surprisingly encountered. As the lowest part of the Berchem Formation, the Edegem Member, was dated as earliest Burdigalian (Louwye et al., 2000), the reworking of these taxa within this sample of the Kiel Member cannot be excluded, although this was not clear from the dinocyst preservation.
- S2 is a *Glycymeris* shell bed of ca. 20–25 cm thickness in the lower part of the Antwerpen Member. The shells show little or no signs of abrasion. Although most shells are unarticulated and oriented convex upwards, concave-up oriented valves and articulated specimens occur to a lesser extent. This bed is characterized by the presence of largely authigenic phosphatic concretions (Figures 7d and 8d). This horizon is informally referred to as the *Haustator eryna* phosphatic horizon, as *Haustator eryna* (D'Orbigny, 1852) is replaced by *Turritella subangulata* (Brocchi, 1814) in the higher shell beds. The bed lies about 1 m above the base of the Antwerpen Member in the northern part of the study area and overall converges towards the base in the southern direction. For example, in the southern Posthofbrug and Post X outcrops, the phosphatic level lies only a few centimetres above the basal shell bed of the Antwerpen Member, with which it seems to have merged (Everaert et al., 2020; Hoedemakers & Dufraing, 2018). In contrast, S2 lies ca. 50 cm above the base of the Antwerpen Member in the Argenta outcrop. This level was dated as early Langhian by Louwye et al. (2000, 2010) and Everaert et al. (2020), as dinocyst biozone DN4 of de Verteuil and Norris (1996) could be recognized.
- S3 is one of the most obvious shell beds, recognized in the top of the Antwerpen Member in the southernmost outcrops of the profile, and informally referred to as "*Glycymeris* crag" ("*Glycymeris* bank" in Hoedemakers & Dufraing, 2018). This relatively compact, massive layer consists of several decimetres of *Glycymeris* shell accumulations (Figure 7c). The thickness of this layer increases

from several decimetres in the south towards 1 m or even more in the northern part of the correlation panel. Most disarticulated valves are convex-up orientated, articulated specimens are more concentrated at the base of the crag. Locally, the shell crag can show two to three breaks of a few centimetres of sediment without *Glycymeris* valves, making the *Glycymeris crag* appear to split into multiple closely interspaced shell beds. However, this internal architecture of the *Glycymeris* crag is highly variable. Because of these characteristics, this shell bed was interpreted as a storm deposit by Hoedemakers and Dufraing (2018). In most outcrops, dispersed *Panopea* in life position are often present just below the base of the *Glycymeris* crag. To the south of the Borgerhout district, the *Glycymeris* crag is consistently described by Hoedemakers and Dufraing (2018) and Everaert et al. (2020) at about 1–2 m above the base of the Antwerpen Member. In the more northern outcrops at the Borgerhout district, where the base of the Antwerpen Member was not reached, there is no specific mention of the *Glycymeris* crag. On the drawings and descriptions by De Meuter et al. (1976), however, a compact, thick accumulation of shells could be recognized also in the outcrops in Borgerhout, at the suspected stratigraphic level (Figures 6 and 12). Consequently, we were able to correlate the *Glycymeris* crag with all the different outcrops of this study. The *Glycymeris* crag was attributed to the early Langhian dinocyst biozone DN4 at the

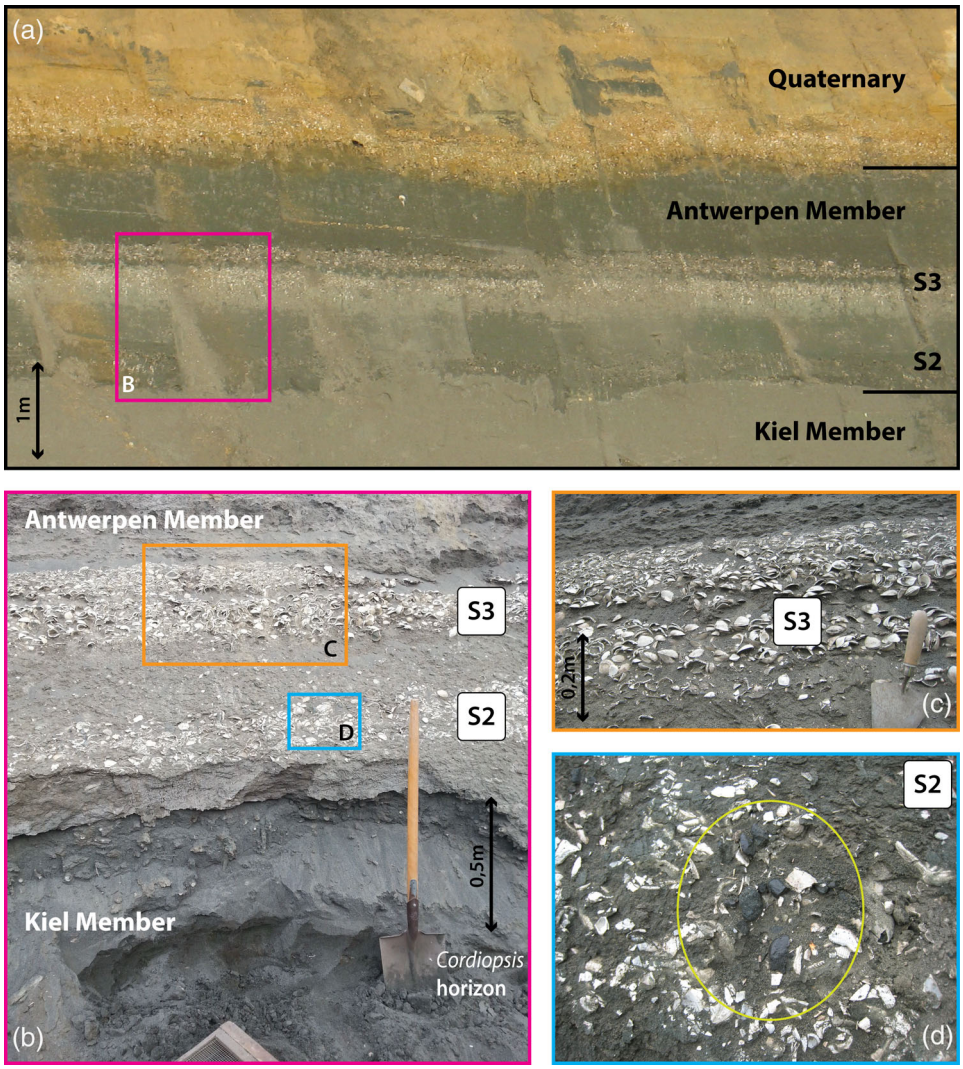

FIGURE 7 (a) The expression of the uppermost part of the Kiel Member and the Antwerpen Member in outcrops. Notice the darker colour of the Antwerpen Member compared to the Kiel Member in the uppermost section. The S2 and S3 shell beds in the Antwerpen Member are indicated. Notice the continuation of S3 across the entire outcrop as a thick shell bed. Temporary Posthofbrug outcrop, photo by Pieter De Schutter (January 2008). (b) Close-up view of the (weathered) boundary between the Antwerpen and Kiel Members, again with shell beds S2 and S3 indicated. Note the lithified burrows in the top of the Kiel Member, and the base of the Antwerpen Member overhanging the Kiel Member as the latter is less erosion resistant due to its relatively lower clay content. Temporary Post X outcrop, photo by Pieter De Schutter (August 2015). In the right lower corner, there is a further zoom view on the S2 and S3 shell beds (both Post X outcrop, August 2015). (c) Level S3 consists of thousands of densely packed, disarticulated valves of *Glycymeris baldii*, mostly convex-up oriented. (d) Within the S2 level, a concentration of black phosphorites is marked by a yellow circle. The shells are fragmented by mechanical damage and by weathering due to long-term exposure to the weather in the outcrop. The encircled section is about 10 cm in diameter

FIGURE 8 (a) Sandstone-bearing level Z2 covered by 2 m of loose, grey, bioturbated coarse sand of the Kiel Member. The sandstones are indicated by the white encirclements and are just overlying a thin horizon of decalcified shells. Temporary Argenta outcrop (April 2019). (b, c) represent, respectively, the top and base of a shelly sandstone block from this sandstone-bearing level Z2 (collection IRSNB 7697) in the Kiel Member. (d) Several examples of bioeroded Lamnidae shark teeth (1–4, 7) and phosphate nodules (6, 8, 9) from the phosphatic horizon S2 in the lower part of the Antwerpen Member. Note the (sub)tropical coral *Flabellum* cf. *tuberculatum* embedded in nodule 8, and the phosphatic concretion covering the root of *Carcharodon hastalis* no. 5 (temporary Posthofbrug outcrop, coll. Pieter De Schutter). (e) Illustration of the stronger abrasion of shells in the Kiel Member (lower shell) compared to the Antwerpen Member (upper shell). In addition, *Glycymeris* from the Kiel Member generally show a more symmetric morphology with less posterior elongation, probably adapted to rougher, more current swept sea bottoms (temporary Argenta outcrop, see Everaert et al., 2020)

Borgerhout-Rivierenhof and Posthofbrug outcrops by Louwye et al. (2000, 2010; Figure 12).

- S4 is a thin, well-developed shell bed that is located less than 50 cm above S3 in the Borgerhout-Rivierenhof and Borgerhout-Stenen Brug outcrops (sample 11 in De Meuter et al., 1976; Figures 6 and 12). This layer was not recognized in the Tweelingenstraat outcrop by Everaert et al. (2020), where it may have converged into S3. The correlation of this layer is uncertain. This shell bed falls within the top of the early Langhian dinocyst DN4 biozone at the Borgerhout-Rivierenhof section (Louwye et al., 2000; Figure 12).
- S5 lies 1.5 and 2.5 m above the S3 in the Borgerhout-Rivierenhof (sample 15 in De Meuter et al., 1976; Figure 12) and Borgerhout-Stenen Brug outcrops (Figure 6), respectively. Like the S3 *Glycymeris* crag, it is a massive, compact shell bed mainly consisting of *Glycymeris*. This shell bed was not recognized in the Tweelingenstraat outcrop, probably as the result of postdepositional erosion. Like S4, the correlation of this layer is rather uncertain. This shell bed lies within the early Langhian to early Serravallian DN5 dinocyst biozone (Louwye et al., 2000; Figure 12).

At the top of the Antwerpen Member in the Borgerhout outcrops, a hardground was identified by De Meuter et al. (1976), which is herein identified as H1 (Figure 12).

In the Berchem-Grote Steenweg outcrop, the S3 *Glycymeris* crag forms the top of the Antwerpen Member below the erosive Quaternary base (Figure 5). The Antwerpen Member thickens as its base deepens in a northern direction. In the northern part of our profile at the Borgerhout district, the Antwerpen Member reaches thicknesses and depths of more than 8 m. As the result of this large increase in thickness and depth, the underlying Kiel Member is supposedly no longer exposed by the outcrops described by De Meuter et al. (1976) in the Borgerhout district. We, however, doubt this interpretation because of the following observations (Figure 6):

- The lowermost 1.5 m of the Borgerhout-Stenen Brug outcrop is drawn as coarser sand with bioturbation, which is typical for the entire Kiel Member.
- Higher up, sample 1 is described as a thin shell bed with loose *Glycymeris* valves, sometimes in a convex-up position. This bed might be correlated to the *Glycymeris-Cyrtodaria* horizon of Everaert et al. (2020). However, sandstones on top of the shell bed are lacking. Unfortunately, this correlation remains very uncertain, as samples are lacking.
- 1.5 m higher up in this outcrop, a sample (2) is described as a thin shell bed with clay streaks and sandstones at its base. This description is characteristic feature for the base of the Antwerpen Member as observed in other outcrops (see Everaert et al., 2019, 2020; Hoedemakers & Dufraing, 2018; Louwye et al., 2010; Figure 3).
- Another 1 m higher in the same outcrop (samples 3, 4, and 5), S2 is interpreted by this study (*Haustator eryna* is mentioned in sample 4). Two meters higher, also the characteristic compact, a thick accumulation of *Glycymeris* shells of S3 occurs, with *Panopea* just underneath S3.

Based on these observations, we suggest to reinterpret the basal 3 m of the Borgerhout-Stenen Brug outcrop as the Kiel Member, below almost 9 m of the Antwerpen Member (Figure 6). Especially, the lower 1.5 m of the section can be attributed with certainty to the Kiel Member. According to this reinterpretation, the Kiel Member is only unexposed in the northernmost outcrop of the correlation panel, namely Borgerhout-Rivierenhof. The shell bed with sandstones in the

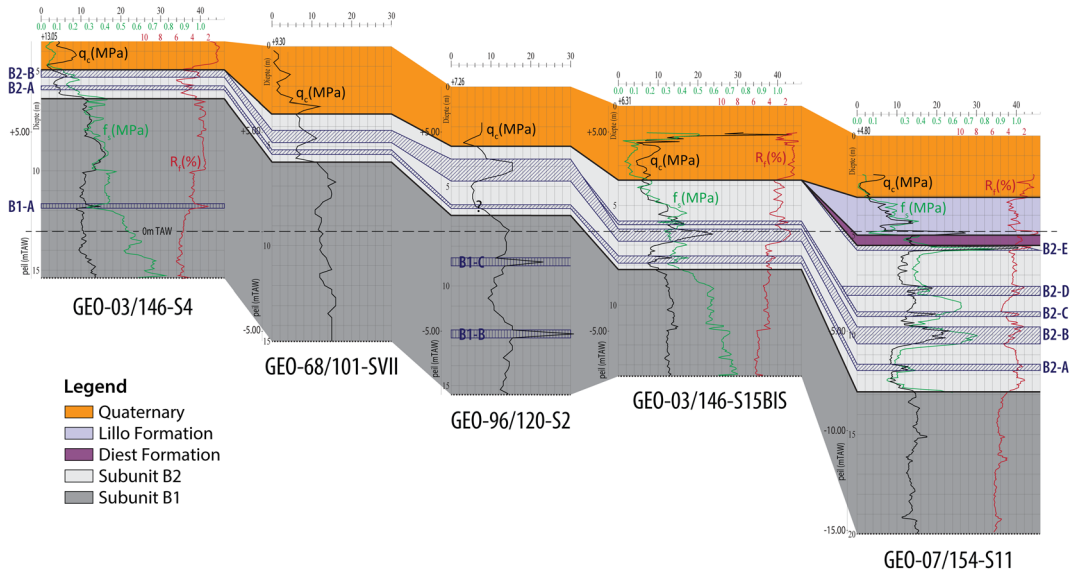

FIGURE 9 S-N CPT correlation profile of the Miocene to Quaternary units along the east of the city of Antwerp based on CPTs. The Berchem Formation is subdivided into geotechnical subunits (B1 and B2) and horizons (B1-A to -C and B2-A to -E). For the location of the CPTs of this profile, see Figure 1

basal sample of the latter outcrop most likely represents the base of the Antwerpen Member.

4 | GEOTECHNICAL STRATIGRAPHY

The Berchem Formation in the southern Antwerp City area is typically present on top of the lower Oligocene Boom Formation and below continental Quaternary strata (Figure 9). Further, towards the north, a thin interval of the Upper Miocene Diest Formation and/or Lower Pliocene Kattendijk Formation is intercalated between the Berchem Formation and Quaternary strata (cf. De Meuter et al., 1976).

In the selected CPTs in the eastern Antwerp City area, the base of the Berchem Formation or Boom Formation was not reached (Figure 9). Instead, the CPTs ended in either the Kiel or Edegem members of the Berchem Formation. As this study focused on the boundary between the Antwerp and Kiel Members, the CPTs in our profile are cut off within the Kiel Member.

The upper boundary of the Berchem Formation with the superjacent Quaternary is typically expressed by a marked decrease in q_c values and—if available—R_f values. More to the north, the upper boundary of the Berchem Formation with the Kattendijk Formation is expressed by an increase in q_c values and a decrease towards uniform R_f values, according to Deckers and Louwye (2020; Figure 4). In our profile along the eastern Antwerp City area, the typical CPT expression of the Kattendijk Formation was not encountered, probably because it is too thin (<0.5 m) or locally absent due to postdepositional erosion. In the uppermost section of the northernmost CPT, low q_c and high R_f values are present which most likely represent the clayey part of the Lillo Formation (see also Deckers, Louwye, & Goolaerts, 2020). The underlying q_c spike could represent a shell accumulation at the base of the Lillo Formation. The section below this q_c spike and the underlying q_c spike might represent the facies of the Deurne Member of the Diest Formation. In this area, the Deurne Member is indeed present between 0 and −1 m TAW according to the outcrop interpretations by De Meuter et al. (1976). The R_f values for the Deurne Member are slightly lower than for the upper part of the Berchem Formation (Antwerpen Member), which is consistent with the lower glauconite content of the first compared to the latter as known from the literature (cf. Adriaens, 2015).

On their CPT correlation panel along the northern margin of the city of Antwerp, Deckers and Louwye (2020) identified a geotechnical twofold subdivision within the Berchem Formation. A lower part (subunit B1) with relatively higher q_c—and R_f values compared to an upper part (subunit B2; Figure 4). At the boundary between both subunits of the Berchem Formation, a reference horizon BL1 was defined. On the correlation panel of this study, we recognized a very similar twofold subdivision for the Berchem Formation. In the study area, subunit B1 shows rather uniform q_c values of around 12–14 MPa, and R_f values generally increase downwards from 3 to 4% in the upper part up to 6% in the lower parts. The uppermost 2–4 m of subunit B1 often shows the highest q_c values and lowest R_f values. Locally, small (in the order of decimetres) spikes in q_c values were observed within subunit B1, which reached values of 20–30 MPa, and are indicated in this study as B1-A, -B, and -C (Figure 9).

Subunit B2 shows background q_c values in the order of 8 MPa, and R_f values around 3–4%. Within the low background q_c values, several q_c spikes which coincide with R_f minima can be recognized across the study area. In the northern part of the profile, at 0.5–1.5 m above the base of the subunit, a small q_c-spike can be observed with values around 12–14 MPa, hereafter referred to as B2-A (Figure 9). This horizon disappears as it thins towards the south. In the northernmost parts, this horizon had widened into a zone of 1-m thickness which comprises two small spikes.

Higher up, at about 1 m (in the south) to 3 m (in the north) above the base of subunit B2, a larger q_c-spike with values of up to 24 MPa is visible on all CPTs. This spike, hereafter referred to as B2-B, increases in thickness from less than 0.5 m in the south, where it is covered by the Quaternary, towards over 1 m in the northern part of the profile.

Northwest of the study area, along Figure 5 of Deckers and Louwye (2020; Figure 4), the q_c spikes of B2-A and B2-B can also be identified in the top of the Berchem Formation.

On top of B2-B in subunit B2, several other q_c spikes can be observed on CPT GEO-07/154-S11 (Figure 9). The most obvious spikes were called B2-C, -D, and -E. Spike B2-C could be correlated towards the more southern CPT GEO-03/146-S15BIS, but the others could not, partly due to stronger erosion of the top of subunit B2 in the latter CPT, but probably also as the result of changes in CPT signature between both CPTs.

5 | CORRELATION BETWEEN OUTCROPS AND GEOTECHNICAL STRATIGRAPHY

The combination of the outcrop correlation profile of Figure 5 with the CPT correlation profile of Figure 9 provides the new correlation profile of Figure 10. The latter figure provides the correlation between the geotechnical stratigraphy on CPTs with the lithostratigraphic units and layers as described within the outcrops. Figures 11 and 12 provide further detail on this correlation at the Argenta and Borgerhout-Rivierenhof outcrops.

Figure 10 shows that CPT subunit B1 corresponds to the Kiel Member, whereas CPT subunit B2 corresponds to the Antwerpen Member. The overall higher q_c values for the Kiel Member (CPT subunit B1) compared to the Antwerpen Member (CPT subunit B2) are probably the result of the coarser and less clayey nature of the sands in the first unit compared to the latter unit, which are the main criteria used to distinguish these units in the outcrops (cf. Everaert et al., 2020). According to the latter study, the boundary between the Antwerpen and Kiel Members is sharp, which corresponds to the abrupt decrease in q_c values from subunit B1 towards subunit B2. Contrary to the q_c values, the R_f values show no consistent pattern change from the Kiel Member towards the Antwerpen Member in the study area, which is probably due to lateral and vertical variations in

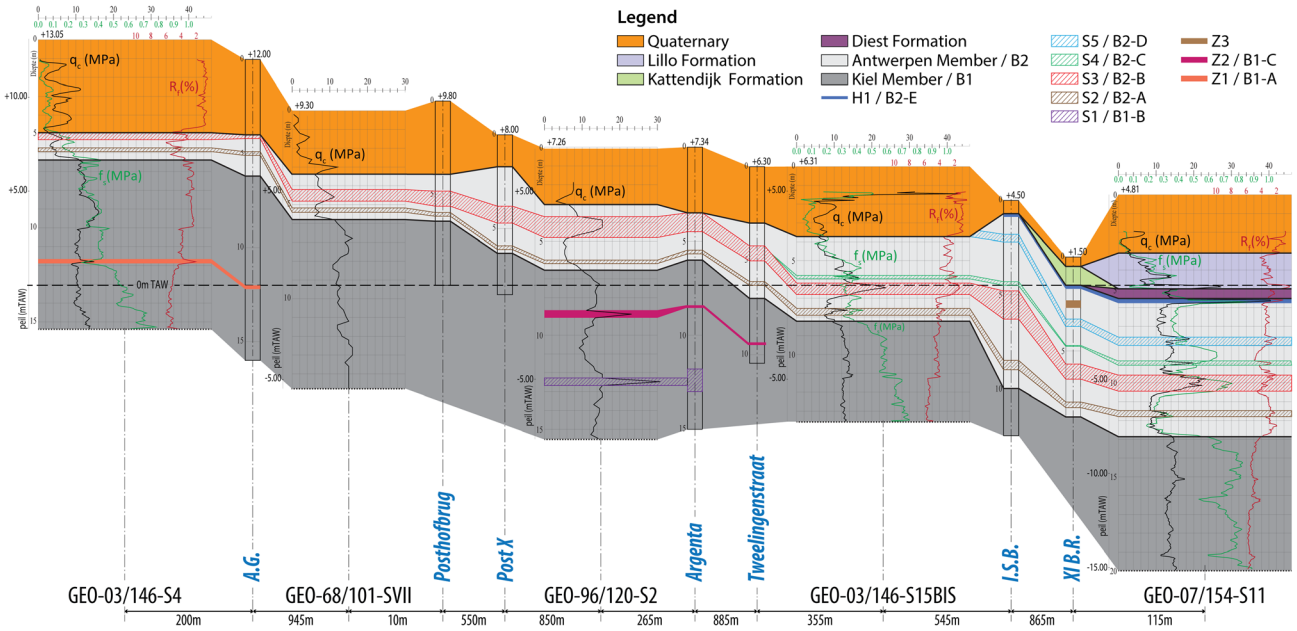

FIGURE 10 S-N correlation profile between temporary outcrops (Figure 5) and CPTs (Figure 9) along the east of the city of Antwerp. For the location of the profile, see Figure 1

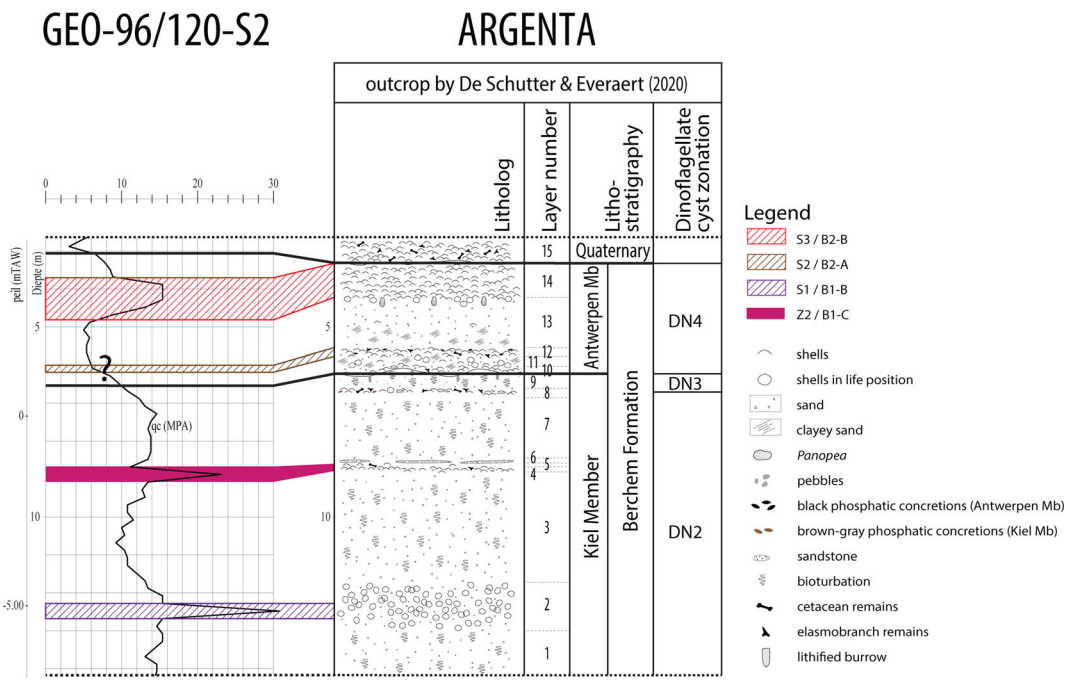

FIGURE 11 A closer look at the correlation between the Argenta outcrop as described and drawn by De Schutter and Everaert (2020) and a nearby mechanical CPT. Everaert et al. (2020) performed dinocyst analyses on samples of this outcrop and thereby established the biozones as defined by de Verteuil and Norris (1996), shown on the right-hand side. For the location of the outcrop and CPT, see Figure 1

clay and/or glauconite content. Further analyses of the glauconite content and grain-size distributions in both members in the Antwerp area are needed to understand the changes in R_f patterns.

Within the Antwerpen and Kiel Members, several q_c spikes numbered in this study can be correlated with shells beds, horizons with sandstones, and hardgrounds, as observed in the nearby outcrops at more or less corresponding depths:

Within the Kiel Member (CPT subunit B1), three q_c spikes (B1-A to -C) were marked by this study. B1-A correlates with a level Z1 that contains sandstones in the Berchem-Grote Steenweg outcrop as

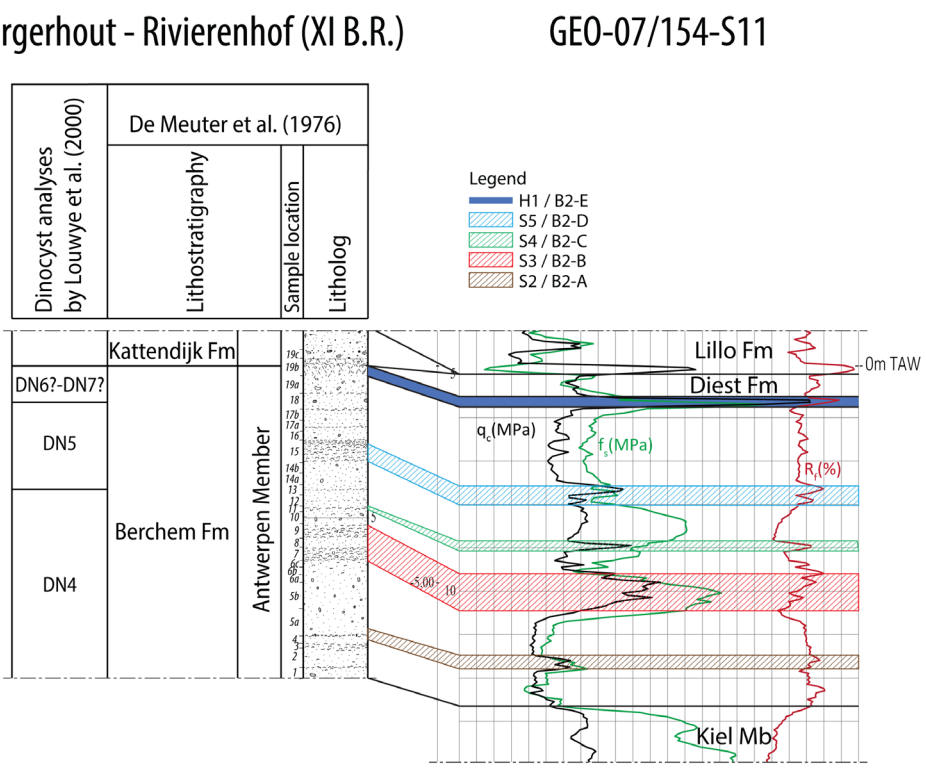

FIGURE 12 A closer look at the correlation between the Borgerhout-Rivierenhof temporary outcrop as described and drawn by De Meuter et al. (1976) and a nearby electric CPT. Louwye et al. (2000) performed dinocyst analyses on samples of this outcrop and thereby established the biozones as defined by de Verteuil and Norris (1996), shown on the left-hand side. For the location of the outcrop and CPT, see Figure 1

described by De Meuter et al. (1976). B1-C correlates with level Z2 that contains shelly, glauconitic sandstones in the Argenta and Tweelingenstraat outcrops as described by De Schutter and Everaert (2020) and Everaert et al. (2020; Figure 11). q_c spike B1-B correlates to shell bed S1 in the Argenta outcrop, but since this q_c spike is much thinner than S1 (0.1 m vs. c. 1.2 m), B1-B probably correlates to a dense shell band within S1 or to a dispersed sandstone within this shell level.

The CPTs and outcrops indicate that the sandstone and shell bands in the Kiel Member only have a local occurrence and cannot be traced across the entire study area.

It is noteworthy that the *Cordiopsis* horizon (see Figure 7b), described from both the Post X and Argenta outcrops (De Schutter & Everaert, 2020; Everaert et al., 2019, 2020), could not be recognized in the nearby CPTs GEO-68/101-SVII and GEO-96/120-S2. In both temporary outcrops, it was located 0.5 m below the (erosional) base of the Antwerpen Member, at the transition between dinocyst biozones DN2 and DN3. At the Berchem-Grote Steenweg, the dinocyst biozone DN2/3 boundary coincides with Z1, but the lithology of this level described by De Meuter et al. (1976) differs somewhat from the observations at the Post X and Argenta outcrops. As the *Cordiopsis* horizon consists in these sections of winnowed (bio)clasts (brown-grey phosphatic concretions, shark teeth, cetacean remains, strongly decalcified shells, sandstone chunks at the base) which are locally concentrated in lenses with varying thicknesses, this horizon can be easily missed on CPTs. The absence of this level in the more north-east located electrical CPT GEO-03/146-S15BIS is not surprising, as the base of the Antwerpen Member seems to cut deeper into the underlying Kiel Member, probably removing the *Cordiopsis* horizon and the entire DN3 dinocyst biozone in the nearby Tweelingenstraat outcrop (Everaert et al., 2020). This is most likely also the case in the nearby Kievitstraat section (Louwye et al., 2000).

Within the Antwerpen Member, five q_c spikes, called B2-A to -E, were observed. The B2-A q_c spike correlates with shell bed S2, which represents a thin layer of shell accumulations with phosphorite nodules, that was yet identified as the informally-called "*Haustator eryna* phosphatic horizon" in the Post X, Argenta, and Tweelingenstraat outcrops by Everaert et al. (2020; Figure 11). This shell bed was observed in all the outcrops at about a few decimetres to 1 m above the base of the Antwerpen Member.

B2-B is the thickest q_c spike on the correlation profile. It shows a good correlation with shell bed S3, also referred to as *Glycymeris* crag (Figures 11 and 12). This accumulation of *Glycymeris* shells is generally between 0.5 and 1 m thick and is often described as compact, which explains why it is expressed by a strong, thick q_c spike. Because of its thickness and lateral continuity, this horizon forms an excellent marker horizon on the CPTs as well as in outcrops.

In the northernmost CPT GEO-07/154-S11 of the correlation profile, the Antwerpen Member is thickly developed and shows several more q_c spikes above the *Glycymeris* crag. These spikes most likely correlate to shell beds in the nearby Borgerhout-Rivierenhof outcrop as described by De Meuter et al. (1976; Figure 12). Spikes B2-C and -D can indeed tentatively be correlated with shell beds S4 and S5 in both the Borgerhout-Rivierenhof and -Stenen Brug outcrops. It seems likely that—as the units thin in a southern direction—shell bed S4 becomes part of the S3 *Glycymeris* crag in the Tweelingenstraat outcrop. Shell bed S5 is absent south of the Borgerhout-Stenen Brug outcrop due to post-depositional erosion. The uppermost spike B2-E possibly correlates to a hardground in the top of the Antwerpen Member as

described in the Borgerhout-Rivierenhof outcrop (Figure 12). In the latter outcrop, the Antwerpen Member reaches a thickness of about 8 m underneath the Kattendijk Formation. On the nearby CPT GEO-07/154-S11, no indications were found for the Kattendijk Formation, but instead, the Diest and Lillo Formations are thought to overly the Antwerpen Member, albeit a very uncertain interpretation.

6 | REGIONAL SIGNIFICANCE

The results of this study show that the boundary between the Antwerpen and Kiel Members could be established very well by means of both electric and mechanical CPTs, and this is both in northern and southern Antwerp. This is probably the result of the more fine-grained nature and more clayey admixture within the lower part of the Antwerpen Member, causing a lowering of the q_c values compared to the coarser-grained Kiel Member. However, grain-size analyses should be performed in the future to confirm and quantify granulometric differences.

The boundary between the Antwerpen and Kiel Members was dated by means of dinocyst species as the latest Burdigalian by Louwye et al. (2000; Figure 2), which was later on confirmed by Everaert et al. (2020; Figure 11). The latest Burdigalian thus forms an important shift towards finer facies, indicating a transgression (Louwye, 2005). As the coastline shifted further landward towards the south, causing a larger distance to the coast and probably a lower energetic depositional environment, more fine-grained sediments reached the Antwerpen city area. Hence, the more clayey admixture in the basal part of the Antwerpen Member. The lower energetic depositional environment for the lower Antwerpen Member compared to the Kiel Member is also in accordance with the stronger abrasion of shells in the Kiel Member, which points to a higher energetic habitat above the storm wave base. Moreover, the more symmetric morphology of *Glycymeris* in the Kiel Member is probably also an adaptation to a rougher, shallower environment (Everaert et al., 2020; Figure 8e). Lower energetic levels in the basal Antwerpen Member also probably resulted in lower sedimentation rates, as shown by the presence of (at least partially) authigenic phosphorites (Figures 7d and 8d) and glauconites (Adriaens, 2015), and bioeroded Lamnidae shark teeth (Figure 8d) in shell bed S2 of the Antwerpen Member (Everaert et al., 2020). A rough estimate of the sedimentation rates can be calculated for the study area:

- According to our CPT interpretation and correlation with the Borgerhout-Rivierenhof outcrop nearby, the Antwerpen Member is about 9-m thick in the Borgerhout district. According to dinocyst analyses of samples from this outcrop by Louwye et al. (2000; Figure 12), the Antwerpen Member has an early Langhian to middle Serravallian age here. The 9 m of sediment was therefore deposited during a time span of more than 2.8 Myr (13.2–16 Ma based on Figure 6 of Louwye et al., 2020; Figure 2). This gives a sediment accommodation rate (without compensating for compaction) of less than 3.2 m/Myr, without implying that this rate was continuous within the entire time interval of the biozones.
- The underlying Kiel and Edegem members were deposited during a similar time span (16–19 Ma based on Figure 6 of Louwye et al., 2020). According to the most recent geological model of Van Haren et al. (2021), the base of the Berchem Formation lies at a depth of about −31 m TAW underneath the Borgerhout district. The combined Edegem and Kiel Members are consequently 23-m thick (−8 to −31 m TAW) in the latter area. This gives a sediment accommodation rate (without compensating for compaction) of 7.8 m/Myr, or more than double that of the Antwerpen Member, without implying that this rate was continuous. In reality, however, the sediment accommodation rate of the Kiel and Edegem members will be even higher, as the late Burdigalian dinocyst biozone DN3 in the upper part of the Kiel Member seems to disappear completely in northern Antwerp (Everaert et al., 2020; Louwye et al., 2000). Taking the disappearance of DN3 into account, maximum accommodation rates in the direction of 23 m/Myr may be estimated for the Borgerhout district (northern Antwerp).

This shows that within the Antwerpen city area, the sedimentation rates are at least more than halved from the Burdigalian (Edegem and Kiel Members) towards the Langhian (Antwerpen Member). In their study of biostratigraphically analysed boreholes in the Campine area, Deckers and Louwye (2019) also noticed a decrease in sediment accumulation rates from the Burdigalian towards the Langhian and Serravallian. Even further northeast, in the northern Roer Valley Graben, the middle Miocene Groote Heide Formation (largely time equivalent to the Antwerpen Member; Figure 2) shows higher gamma-ray values, probably also as the result of the more clayey nature and increase in glauconite content, compared to the underlying lower Miocene top of the Veldhoven Formation (largely time equivalent to the Edegem and Kiel Members; Everaert et al., 2020; Munsterman et al., 2019; Figure 2). This shows that the observed fining from the Kiel Member towards the Antwerpen Member in the Antwerpen area is part of a regional facies change, which was referred to by Munsterman et al. (2019) as the EMU (in Figure 2). Deckers and Munsterman (2020) associated the start of this regional transgression with the start of the Mid-Miocene Climatic Optimum. Everaert et al. (2020) indeed showed that the EMU lies at the boundary between the Antwerpen and Kiel Members, as the entire late Burdigalian (DN3) gradually disappears towards northern Antwerpen, leaving a hiatus spanning ca. 2 Ma.

Maximum flooding was estimated to have been reached at shell level S2 (q_c spike B2-A) just above the base of the Antwerpen Member ("*Haustator eryna* phosphatic horizon"), as this level contains a relatively high number of the neritic dinoflagellate cyst genus *Spiniferites* and very low numbers of shallow to restricted marine *Paralecaniella* spp. compared to adjacent assemblages in the succession (Everaert et al., 2020). Maximum flooding at this level is in agreement with the low q_c values, reflecting finer grain sizes, of this basal part of the Antwerpen Member surrounding the q_c spike of the level itself (Figure 10). The presence of phosphorites and bioeroded shark teeth as observed by Everaert et al. (2020) (Figures 7d and 8d) in this level is also in agreement with very low sedimentation rates which are

expected at the maximum flooding. After this transgression, the depositional depth decreased again towards an estimated maximum of 50 m (based on the presence of the brachiopod genus *Discinisca*; Hoedemakers & Dufraing, 2018). This decreased depth is also in accordance with the palynological analysis of Louwye et al. (2010) who noticed a strong increase of *Paralecaniella* spp. and a marked decrease of *Spiniferites* in sample PHB-1 (S3 *Glycymeris* crag). The latter authors interpreted these trends as a change from open neritic conditions in the basal part of the Antwerpen Member to shallow to restricted marine environment in S3. This shallowing trend can also be deduced directly from the lithology, as a gradual upward decrease of the clay content was observed between S2 and S3 in multiple outcrops (Everaert et al., 2019; Hoedemakers & Dufraing, 2018).

Our correlation profile shows that for the Antwerpen Member, the shell beds and sandy units in between them thin in the southern direction (Figure 10). The interval between the *Glycymeris* crag in the Antwerpen Member and the base of the Antwerpen Member thins from 3 m in the north to only 1 m in the south. This indicates a decrease in accommodation space for the Antwerpen Member in a southern direction.

ACKNOWLEDGEMENTS

This article was constructed within the framework of a project called "Geological questions for the Neogene" for the VLAKO-reference task as ordered by the Bureau for Environment and Spatial Development—Flanders, VPO. We are grateful to Katrien De Nil, Jan van Roo and Jasper Verhaegen from VPO for the fruitful collaboration that made the work on this project possible. The same persons are also thanked, together with Ilse Vergauwen and Chandra Algoe (MOW), Stijn Huyghe (CIVIEL), and Michiel Dusar, for the constructive discussions that shaped this article. Katrijn Dirix (VITO) is thanked for database support and Katleen van Baelen (VITO) is thanked for her excellent work on the figures. S.E. wants to thank Dirk Munsterman (TNO), Kristiaan Hoedemakers (RBINS), Pieter De Schutter (RBINS), and Taco Bor (Sliedrecht, the Netherlands) for stimulating discussions on the Berchem Formation. The latter two researchers are also thanked for providing some photographs for this paper. Finally, we also thank both reviewers, Stephen Louwye (UGent) and Dirk Munsterman (TNO) for their constructive suggestions, which improved our paper.

PEER REVIEW

The peer review history for this article is available at https://publons.com/publon/10.1002/gj.4384.

DATA AVAILABILITY STATEMENT

The data that support the findings of this study are available from the corresponding author upon reasonable request.

ORCID

Jef Deckers https://orcid.org/0000-0002-5373-8733
Stijn Everaert https://orcid.org/0000-0001-9551-9275

REFERENCES

Adriaens, R. (2015). *Neogene and Quaternary clay minerals in the southern North Sea* (Unpublished Ph.D. Thesis). KU Leuven, Leuven. p. 272.

Brocchi, G. (1814). *Conchiologia fossile subapennina con osservazioni geologiche sugli Apennini e sul suolo adiacente: Tomo secondo* (pp. 1–712). Milan, Italy: Stamperia Reale.

Deckers, J., & Louwye, S. (2019). Late Miocene increase in sediment accommodation rates in the southern North Sea Basin. *Geological Journal*, *55*, 728–736.

Deckers, J., & Louwye, S. (2020). The architecture of the Kattendijk Formation and the implications on the early Pliocene depositional evolution of the southern margin of the North Sea Basin. *Geologica Belgica*, *23*(3–4), 323–331. https://doi.org/10.20341/gb.2020.017.

Deckers, J., De Koninck, R., Bos, S., Broothaers, M., Dirix, K., Hambsch, L., … Van Haren, T. (2019). *Geologisch (G3Dv3) en hydrogeologisch (H3D) 3D-lagenmodel van Vlaanderen. Studie uitgevoerd in opdracht van het Vlaams Planbureau voor Omgeving, departement Omgeving en de Vlaamse Milieumaatschappij*. Report prepared by the VITO, Mol, VITO-rapport 2018/RMA/R/1569. p. 286. Retrieved from https://archief-algemeen.omgeving.vlaanderen.be/xmlui/handle/acd/251494

Deckers, J., Louwye, S., & Goolaerts, S. (2020). The internal division of the Pliocene Lillo Formation: correlation between cone penetration tests and lithostratigraphic type sections. *Geologica Belgica*, *23*(3–4), 333–343. https://doi.org/10.20341/gb.2020.027.

Deckers, J., & Munsterman, D. (2020). Middle Miocene depositional evolution of the central Roer Valley Rift System. *Geological Journal*, *55*(9), 6188–6197. https://doi.org/10.1002/gj.3799.

De Nil, K., De Ceukelaire, M., & Van Damme, M. (2020). A reference dataset for the Neogene lithostratigraphy in Flanders, Belgium. *Geologica Belgica*, *23*(3–4), 413–427. https://doi.org/10.20341/gb.2020.021.

De Meuter, F. J., & Laga, P. G. (1976). Lithostratigraphy and biostratigraphy based on benthonic foraminifera of the Neogene deposits in northern Belgium. *Bulletin van de Belgische Vereniging voor Geologie/Bulletin de la Société belge de Géologie*, *85*, 133–152.

De Meuter, F., Wouters, K., & Ringele, A. (1976). Lithostratigraphy of Miocene sediments from temporary outcrops in the Antwerp City area. *Professional Papers du Service géologique de Belgique*, *3*, 1–19.

De Schutter, P., & Everaert, S. (2020). A megamouth shark (Lamniformes: Megachasmidae) in the Burdigalian of Belgium. *Geologica Belgica*, *23*(3–4), 157–165. https://doi.org/10.20341/gb.2020.001.

de Verteuil, L., & Norris, G. (1996). Miocene dinoflagellate stratigraphy and systematics of Maryland and Virginia. *Micropaleontology*, *42*, 1–172. https://doi.org/10.2307/1485926.

D'Orbigny, A. (1852). *Prodrome de Paléontologie stratigraphique universelle des animaux mollusques & rayonnés, faisant suite au cours élémentaire de paléontologie et de géologie stratigraphique: Troisième volume* (pp. 1–189). Paris: Victor Masson.

Dybkjær, K., & Piasecki, S. (2010). Neogene dinocyst zonation for the eastern North Sea Basin, Denmark. *Review of Palaeobotany and Palynology*, *161*, 1–29. https://doi.org/10.1016/j.revpalbo.2010.02.005.

Everaert, S., De Schutter, P., Mariën, G., Cleemput, G., Van Boeckel, J., Rondelez, D., & Bor, T. (2019). Een vroeg-miocene fauna uit het Zand van Kiel (Formatie van Berchem) bij Post X in Berchem (Antwerpen). *Afzettingen WTKG*, *40*, 83–100.

Everaert, S., Munsterman, D., De Schutter, P., Bosselaers, M., Van Boeckel, J., Cleemput, G., & Bor, T. (2020). Stratigraphy and palaeontology of the lower Miocene Kiel Sand Member (Berchem Formation) in temporary exposures in Antwerp (northern Belgium). *Geologica Belgica*, *23*(3–4), 167–198. https://doi.org/10.20341/gb.2020.025.

Gibbard, P. L., & Lewin, J. (2016). Filling the North Sea Basin: Cenozoic sediment sources and river styles. *Geologica Belgica*, *19*, 201–217. https://doi.org/10.20341/gb.2015.017.

Glibert, M., & Van de Poel, L. (1965). Les Bivalvia fossiles du Cénozoïque étranger des collections de l'Institut royal des Sciences naturelles de Belgique. I. *Palaeotaxodontida* et *Eutaxodontida*. *Mémoires de l'Institut royal des Sciences naturelles de Belgique*, *77*, 7–112.

Hoedemakers, K., & Dufraing, L. (2018). Een profiel bij Posthofbrug (Antwerpen). *Afzettingen WTKG*, *39*, 65–80.

Louwye, S. (2005). The Early and Middle Miocene transgression at the southern border of the North Sea Basin (northern Belgium). *Geological Journal*, *40*, 441–456. https://doi.org/10.1002/gj.1021.

Louwye, S., De Coninck, J., & Verniers, J. (2000). Shallow marine Lower and Middle Miocene deposits at the southern margin of the North Sea Basin (northern Belgium): Dinoflagellate cyst biostratigraphy and depositional history. *Geological Magazine*, *137*, 381–394. https://doi.org/10.1017/S0016756800004258.

Louwye, S., Marquet, R., Bosselaers, M., & Lambert, O. (2010). Stratigraphy of an early-middle Miocene sequence near Antwerp in northern Belgium (Southern North Sea Basin). *Geologica Belgica*, *13*, 269–284.

Louwye, S., Deckers, J., Verhaegen, J., Adriaens, R., & Vandenberghe, N. (2020). A review of the lower and middle Miocene of northern Belgium. *Geologica Belgica*, *23*(3-4), 156. https://doi.org/10.20341/gb.2020.010.

Munsterman, D. K., & Brinkhuis, H. (2004). A southern North Sea Miocene dinoflagellate cyst zonation. *Netherlands Journal of Geosciences/Geologie en Mijnbouw*, *83*, 267–285. https://doi.org/10.1017/S0016774600020369.

Munsterman, D. K., & Deckers, J. (2020). The Oligocene/Miocene boundary in the ON-Mol-1 and Weelde boreholes along the southern margin of the North Sea Basin, Belgium. *Geologica Belgica*, *23*(3–4), 127–135. https://doi.org/10.20341/gb.2020.007.

Munsterman, D. K., ten Veen, J. H., Menkovic, A., Deckers, J., Witmans, N., Verhaegen, J., … Busschers, F. S. (2019). An updated and revised stratigraphic framework for the Miocene and earliest Pliocene strata of the Roer Valley Graben and adjacent blocks. *Netherlands Journal of Geosciences*, *98*, e8. https://doi.org/10.1017/njg.2019.10.

Nyst, H., & Westendorp, G. D. (1839). Nouvelles recherches sur les coquilles fossiles de la Province d'Anvers. *Bulletin de l'Académie royale des Sciences et Belles-Lettres de Bruxelles*, *6*(2), 393–414.

Ogg, J. G., Ogg, G., & Gradstein, F. M. (2016). *A concise geologic time scale* (p. 240). Amsterdam: Elsevier. https://doi.org/10.1016/C2009-0-64442-1.

Vandenberghe, N., & Louwye, S. (2020). An introduction to the Neogene stratigraphy of northern Belgium: present status. *Geologica Belgica*, *23*(3–4), 97–112. https://doi.org/10.20341/gb.2020.008.

Van Haren, T., Deckers, J., De Koninck, R., Dirix, K., Hambsch, L. & Van Baelen, K. (2021). *Ondiep geologische 3D lagen- en voxelmodel van de regio Antwerpen*. Report prepared by the VITO, Mol, VITO-rapport 2019/RMA/R/1985.

How to cite this article: Deckers, J., & Everaert, S. (2022). Distinguishing the Miocene Kiel and Antwerpen Members (Berchem Formation) and their characteristic horizons using cone penetration tests in Antwerp (northern Belgium). *Geological Journal*, *57*(6), 2129–2143. https://doi.org/10.1002/gj.4384